Biomaterials 225 (2019) 119516

Contents lists available at ScienceDirect

Biomaterials

journal homepage: www.elsevier.com/locate/biomaterials

# Tissue adhesive hyaluronic acid hydrogels for sutureless stem cell delivery and regeneration of corneal epithelium and stroma

Laura Koivusalo[a], Maija Kauppila[a], Sumanta Samanta[b], Vijay Singh Parihar[b], Tanja Ilmarinen[a], Susanna Miettinen[c], Oommen P. Oommen[b,**], Heli Skottman[a,*]

[a] Eye Regeneration Group, Faculty of Medicine and Health Technology and BioMediTech Institute, Tampere University, Tampere, 33520, Finland
[b] Bioengineering and Nanomedicine Lab, Faculty of Medicine and Health Technology and BioMediTech Institute, Tampere University, Tampere, 33720, Finland
[c] Adult Stem Cell Group, Faculty of Medicine and Health Technology and BioMediTech Institute, Tampere University, Finland & Research, Development and Innovation Centre, Tampere University Hospital, Tampere, 33520, Finland

ARTICLE INFO

*Keywords:*
Hyaluronic acid
Hydrogel
Tissue adhesive
Cell delivery
Cornea regeneration

ABSTRACT

Regeneration of a severely damaged cornea necessitates the delivery of both epithelium-renewing limbal epithelial stem cells (LESCs) and stroma-repairing cells, such as human adipose-derived stem cells (hASCs). Currently, limited strategies exist for the delivery of these therapeutic cells with tissue-like cellular organization. With the added risks related to suturing of corneal implants, there is a pressing need to develop new tissue adhesive biomaterials for corneal regeneration. To address these issues, we grafted dopamine moieties into hydrazone-crosslinked hyaluronic acid (HA-DOPA) hydrogels to impart tissue adhesive properties and facilitate covalent surface modification of the gels with basement membrane proteins or peptides. We achieved tissue-like cellular compartmentalization in the implants by encapsulating hASCs inside the hydrogels, with subsequent conjugation of thiolated collagen IV or laminin peptides and LESC seeding on the hydrogel surface. The encapsulated hASCs in HA-DOPA gels exhibited good proliferation and cell elongation, while the LESCs expressed typical limbal epithelial progenitor markers. Importantly, the compartmentalized HA-DOPA implants displayed excellent tissue adhesion upon implantation in a porcine corneal organ culture model. These results encourage sutureless implantation of functional stem cells as the next generation of corneal regeneration.

## 1. Introduction

Millions of people worldwide suffer from corneal blindness [1,2]. Severe corneal blindness resulting from thermal or chemical burns, is characterized by the loss of limbal epithelial stem cells (LESCs), the tissue-resident stem cells of the cornea, which leads to chronic inflammation, overgrowth of blood vessels and conjunctival cells, as well as stromal scarring [3,4]. Currently, these is no treatment available for these patients, as they require the implantation of new functional stem cells for long-term regeneration of the cornea [3,5]. For restoring vision, controlled regeneration of both corneal epithelium and stroma is necessary. Although autologous and allogenic primary LESCs from healthy donor eyes have been widely studied for epithelial regeneration, the supply of isolated stem cells is scarce [6]. With the advancements in stem cell technologies, high quantities of clinically relevant LESCs can be obtained through differentiation from human embryonic stem cells (hESC-LESCs) or induced pluripotent stem cells (iPSCs) for corneal epithelial regeneration [7–10]. For stromal regeneration, one of the most promising cell sources are human adipose stem cells (hASCs), due to their capacity to mitigate inflammation and differentiate into corneal stromal cells post implantation [11–15]. However, delivery of two therapeutic stem cell populations compartmentalized in a tissue-specific arrangement is a daunting task, which we have previously sought to solve by using laser-assisted bioprinting [16]. So far, only few applications have emerged combining different cells to regenerate both the scarred stromal tissue as well as the surface epithelium [17,18], but their implantation requires suturing, which can increase inflammation and neovascularization of the cornea [2].

Hyaluronic acid (HA) is a naturally occurring polysaccharide, which can be chemically modified for many tissue engineering applications, while being enzymatically cleared *in vivo*. We have previously shown the formation of stable HA hydrogels by hydrazone crosslinking between aldehyde and carbodihydrazide derivatives of HA [19,20]. This two-component system allows fast gelation and encapsulation of living

* Corresponding author.
** Corresponding author.
*E-mail addresses:* oommen.oommen@tuni.fi (O.P. Oommen), heli.skottman@tuni.fi (H. Skottman).

https://doi.org/10.1016/j.biomaterials.2019.119516
Received 9 September 2019; Accepted 21 September 2019
Available online 23 September 2019

cells for efficient cell delivery [19–22]. In the cornea, native HA has been shown to induce epithelial cell migration and wound healing, and it has recently been identified as an important regulator of the LESC niche of the cornea, making it an ideal culture substrate for these cells [23,24]. Despite this, no HA based implantable materials for LESC transplantation have been previously reported, as corneal cell attachment to HA based films has been poor [25]. Injectable HA-based materials have previously been used for cell delivery to the corneal stroma [20,26], but these *in situ* forming hydrogels cannot be used to deliver an intact epithelial layer. Hence, new implant design is essential for efficient transplantation of distinctly compartmentalized cells to the cornea, as well as other epithelialized tissues, which require the combination of 3D and 2D cell arrangement.

Sutureless implantation of the hydrogel constructs takes advantage of the tissue adhesive capability of dopamine, a catecholamine derived from marine mussels (*Mytillus edulis*) that functions as a glue in wet conditions [27,28]. Several *in situ* forming tissue adhesive hydrogels based on this catechol chemistry have already been introduced for drug and cell delivery applications [28–30]. However, these hydrogels are formed either through self-polymerization of dopamine residues or metal-coordination polymerization, which both result in the formation of a strong brown coloration unsuitable for corneal applications [28–31]. Thus far, the only previously reported tissue adhesive material with a premade dopamine-containing hydrogel, includes a freeze-dried dopamine-alginate membrane for general surgery applications [32]. In corneal regeneration, dopamine residues can potentially have additional benefits for tissue innervation, as dopamine is a known neurotransmitter of corneal nerves [33].

Thus, our ambition was to develop a tissue adhesive scaffold for corneal regeneration with cellular compartmentalization of LESCs on the surface and hASCs in the hydrogel bulk, promoting regeneration of both the epithelial and stromal layers upon implantation at the defect site. We have successfully developed this compartmentalized scaffold and demonstrated the proof-of-concept of sutureless implantation in a porcine corneal organ culture model, which displayed efficient tissue integration while retaining the functional characteristics of these stem cells.

## 2. Materials and methods

Hyaluronic acid (MW 130 kDa) was purchased from LifeCore Biomedical (Chaska, USA). Dopamine hydrochloride, 1-ethyl-3-(3-dimethylaminopropyl)-carbodiimide hydrochloride (EDC), 1-hydroxybenzotriazole hydrate (HOBt), Carbodihydrazide (CDH), 3-amino-1,2-propanediol and sodium periodate, hyaluronidase (from bovine testes), collagen type IV from human placenta, and 5,5-Dithiobis(2-nitrobenzoic acid) (Ellman's reagent) were purchased from Sigma-Aldrich. Traut's reagent (2-iminothiolane), Zeba™ spin desalting column (7K MWCO), 0.5 M ethylenediaminetetraacetic acid (EDTA, UltraPure), Dulbecco's modified Eagle's medium/Ham's nutrient mixture F-12 (DMEM/F-12 1:1), Advanced DMEM, l-glutamine (GlutaMAX™), amphotericin B, TrypLE™ Select, LIVE/DEAD® viability/cytotoxicity kit, PrestoBlue® reagent, CyQUANT cell proliferation assay and Molecular Probes' secondary antibodies were purchased from Thermo Fisher Scientific. TaqMan primers for keratocan (KERA, Hs00559942_m1), lumican (LUM, Hs00929860_m1), aldehyde dehydrogenase 3A1 (ALDH3A1, Hs00964880_m1) and housekeeping gene GAPDH (Hs99999905_m1), cDNA reverse transcription kit and RNAse free DNase I for qRT-PCR were purchased from Thermo Fisher Scientific. For RNA isolation from hydrogel samples and controls, TRIreagent from Molecular Research Center Inc. (Cincinnati, OH) and RNeasy Mini Kit from Qiagen (Qiagen Sollentuna, Sweden) were used. Synthetic laminin-derived peptides CDPGYIGSR were obtained from Bachem (Bubendorf, Switzerland) and Calbiochem (UK). Antibiotics (100 U $mL^{-1}$ penicillin, 100 µg $mL^{-1}$ streptomycin) and Dulbecco's phosphate buffered saline (DPBS) were purchased from Lonza (Basel, Switzerland). Cell culture media CnT-30 and CnT-Prime-CC were purchased from CELLnTECH (Bern, Switzerland), and human serum (type AB male, HIV tested) from BioWest (Nuaillé, France). Spectra Por-3 dialysis membrane (MWCO 3500 g $mol^{-1}$) used for purification was purchased from Spectrum Lab, USA. All solvents were of analytical quality. Spectrophotometric analyses were carried out on Shimadzu UV-3600 plus UV-VIS-NIR spectrophotometer or PerkinElmer Lambda 35 UV/VIS spectrophotometer.

### 2.1. Synthesis and preparation of hydrogels

#### 2.1.1. Synthesis of dopamine modified hyaluronic acid (HA-DA)

1 mmol of HA (400 mg, 1 equivalent) was dissolved in 60 mL deionized water, to which 1 mmol HOBt (153 mg, 1 equivalent) and 1 mmol dopamine (190 mg, 1 equivalent) was then added. The pH of the reaction solution was adjusted to 5.5 with 1 M HCl and 1 M NaOH. Then 0.25 mmol EDC (48 mg, 0.25 equivalent) was added in 2 batches at 30 min interval. pH of the solution was maintained at 5.5 for 6 h, and then allowed to stir overnight. The reaction mixture was loaded into a dialysis bag and dialyzed against dilute HCl (pH = 3.5) containing 100 mM NaCl (4 × 2 L, 24 h) followed by dialysis in dilute HCl (pH 3.5, 2 × 2 L, 24 h) and then dialyzed against deionized water (2 × 2 L, 24 h). The solution was lyophilized to obtain HA-DA. Degree of dopamine conjugation was 14.4% (with respect to the disaccharide units of HA) as estimated by NMR spectroscopy ($^1$H NMR, 300 MHz). The degree of modification was estimated by calculating the ratio of the N-acetyl peak of HA at 2.0 ppm and the aliphatic protons from dopamine at 2.42 or 2.72 ppm. This estimation was in agreement with the aromatic protons of dopamine between 6.7 and 7.3 ppm (Fig. S1 in Supplementary Information).

#### 2.1.2. Synthesis of HA-CDH conjugate

The conjugation of carbodihydrazide (CDH) on hyaluronic acid was carried out by carbodiimide coupling chemistry following our previously reported protocol [19]. The degree of hydrazide modifications was found to be 10% (with respect to the disaccharide repeat units), as determined by trinitrobenzene sulfonic acid (TNBS) assay [34].

#### 2.1.3. Synthesis of HA-DA-CDH conjugate

The conjugation of carbodihydrazide (CDH) on dopamine-modified hyaluronic acid (HA-DA) was carried out following the same procedure as reported for the synthesis of HA-CDH conjugates. Briefly, 0.5 mmol of HA-DA (200 mg, 1 equivalent) was dissolved in 120 mL of deionized water. Thereafter, 0.375 mmol CDH (34 mg, 0.75 equivalent) and 0.5 mmol HOBt (76.5 mg, 1 equivalent) was added to the aqueous HA-DA solution. The pH of the reaction mixture was adjusted to 4.7. Finally, 0.1 mmol EDC·HCl (20 mg, 0.2 equivalent) was added and allowed to stir overnight. The reaction mixture was dialyzed and lyophilized, as described above. The degree of hydrazide modifications was found to be 10% (with respect to the disaccharide repeat units) as determined using TNBS assay [34].

#### 2.1.4. Synthesis of HA-Aldehyde (HA-Ald)

The HA-Ald was synthesized following our previously developed procedure, as described in Ref. [35]. The percentage of aldehyde modification in HA was found to be 10% (with respect to the disaccharide units) as determined by $^1$H NMR spectroscopy. The modification degree was estimated by treating HA-Ald with *tert*-butyl carbazate followed by NaCNBH3 reduction (Fig. S2 in Supplementary Infromation) [35].

### 2.2. Preparation of hydrogels

The hydrogels were prepared using conventional hydrazone cross-linking chemistry. The individual components were sterilized with UV for 30 min and dissolved to concentration 16 mg $mL^{-1}$ (w/v), HA-Ald

and HA-DA-CDH in sterile DPBS and HA-CDH in sterile 10 wt% sucrose solution. The hydrogels were prepared by mixing the hydrazide component (either HA-CDH or HA-DA-CDH) with HA-Ald in equal volumes. In cell-containing hydrogels, hASCs were suspended in the hydrazide component prior to mixing, at a concentration of $2 \times 10^6$ cells $mL^{-1}$.

### 2.3. Rheological studies

Rheological characterization of the hydrogels was performed to understand the structure-property relationship caused by hydrogel crosslinking chemistry using TA instruments' DHR-II rheometer. Both amplitude and frequency sweep tests were performed to analyze the mechanical properties of the hydrogels. During an amplitude sweep, the amplitude of the deformation was varied while the frequency was kept constant at 1 Hz, to determine the linear viscoelastic region (LVR). Subsequent frequency sweep tests were performed between 0.1 and 10 Hz using a constant strain within the LVR, which was 1% in HA-HA and HA-DOPA gels. For the analysis, the storage and loss modulus were plotted against the frequency (Hz).

The distance between two crosslinks or entanglement points, i.e. the average mesh size (ξ), and average molecular weight between crosslinks ($M_c$) were calculated based on rubber elastic theory that can be applied on hydrogels with elastic character. Average mesh size, ξ, was determined using Equation (1)

$$(\xi) = \left(\frac{G'N}{RT}\right)^{-1/3} \quad (1)$$

where $G'$ is storage modulus of the hydrogel, N is the Avogadro constant ($6.023 \times 10^{23}$ $mol^{-1}$), R is the molar gas constant (8.314 J $K^{-1}mol^{-1}$) and $T$ is the temperature (298 K). Average molecular weight between crosslinks, $M_c$, was calculated using Equation (2)

$$(M_c) = \frac{c\rho RT}{G'_P} \quad (2)$$

where $c$ is the polymer concentration (1.6% w/v), ρ is the density of water at 298 K (997 kg $m^{-3}$), R is the molar gas constant (8.314 J $K^{-1}mol^{-1}$), $T$ is the temperature (298 K) and $G'_p$ is the peak value of $G'$.

DHR-II TA instruments' rheometer was also used to quantify the differences in adhesion properties between HA-HA gels and HA-DOPA gels using a tack adhesion test. We first glued a piece of porcine cornea on the top head of the 12 mm parallel plate and placed a fully cured gel of 2 mm thickness at the bottom parallel plate. Subsequently, the probe (cornea tissue) was placed in contact with the gel, with a holding period of 120 s where a constant force of 100 mN was applied. Thereafter, an axial force of 5 N was applied to separate the probe and the gel at a constant separation rate. The experiment was performed in triplicates and the same probe was used to eliminate the effect of surface roughness and a constant holding period was maintained to establish uniform molecular contacts between the probe and the gel.

### 2.4. Swelling and degradation analysis

To determine the swelling and degradation behavior of the hydrogels, 100 μL hydrogel samples were prepared into cut 1 mL syringes. The initial weight of the samples was recorded and the samples were then submerged in DPBS, hASC culture medium (DMEM/F-12 + 5% human serum) or 20–50 U $mL^{-1}$ hyaluronidase solution. The residual mass of the samples in hyaluronidase were recorded at time points 2 h, 4 h, 6 h, 24 h, 48 h (2 days), 72 h (3 days), and 96 h (4 days) until the samples had degraded. The degradation study was performed for three parallel samples. The hydrogel samples in DPBS and medium were weighed after 6 h, and on following days for a total of three weeks. The swelling measurement was conducted on four parallel samples. The swelling ratio (SR) for the samples was calculated from the recorded weight ($W$) based on Equation (3)

$$SR = \frac{W_{swollen} - W_{initial}}{W_{initial}} \times 100\% \quad (3)$$

### 2.5. Transparency analysis

The transparency of the hydrogels was analyzed based on transmittance properties as well as visual evaluation. The transmittance was measured by preparing the hydrogels in 550 μL micro-cuvettes (light path 10 mm) and measuring their transmittance using a UV/VIS spectrophotometer at wavelengths ranging from 380 to 900 nm, using an empty cuvette (air) as blank. Transmittance was measured from three independent samples. Visual transparency was evaluated from 150 μL hydrogel samples prepared in 10 mm diameter molds. The hydrogel samples were removed from their molds, placed on pieces of text, and photographed from above in natural lighting.

### 2.6. Conjugation of basement membrane proteins

Covalent surface modification of the hydrogels was performed using synthetic laminin-derived peptide CDPGYIGSR and collagen type IV (col IV). Prior to conjugation, the laminin-derived peptide was dissolved in 5% acetic acid at 1 mg $mL^{-1}$, and col IV in 0.25% acetic acid at 2 mg $mL^{-1}$. The final concentrations on hydrogel surfaces were 2 μg $cm^{-2}$ for the laminin peptide, and 5 μg $cm^{-2}$ for col IV. The acidic peptide and protein solutions were brought to pH 8 using 1 M NaOH right before conjugation. Based on the molar concentration of amine groups in col IV (148 μM as determined by TNBS assay), 10-fold molar concentration (1.48 mM) of Traut's reagent was used to convert amines in col IV to thiol groups according to manufacturer's instructions. The thiolated col IV (col IV-SH) was purified using a desalting column with 7K MWCO. The concentration of thiols in the final products was quantified using Ellman's reagent. Thiolated col IV and unmodified col IV were added to the HA-DOPA and HA-HA hydrogels at a concentration of 5 μg $cm^{-2}$, in PBS pH 8.5 containing 1 mM EDTA, and allowed to react at 37 °C for 2 h. Hydrogels without col IV were used as controls. The hydrogels were washed 5 × 5 min with DPBS prior to seeding hESC-LESCs on their surface.

### 2.7. Quantification of thiol groups

The reaction kinetics of the conjugation reaction and the quantification of thiol groups in thiolated col IV were measured using Ellman's reagent. Reaction kinetics were measured using the laminin-derived peptide CDPGYIGSR, which contains only one thiol group in the N-terminal cysteine residue per molecule. The reaction kinetics measurement was performed for the same peptide obtained from two different manufacturers, Bachem and Calbiochem. For quantitation of reaction kinetics, Ellman's reagent was added to the conjugation solution in equal molarity to the amount of peptide. The peptide solution (at a concentration of 2 μg $cm^{-2}$) was pipetted to the gels on a 96-well plate (100 μL per well) and allowed to react for 1 h at RT. The rest of the reaction solution was left as a control to account for the dimerization of the Cys-terminated peptides. Every 10 min, the absorbance of the sample from the hydrogels and from control solution at 412 nm was recorded using the UV/VIS spectrophotometer in 1 mL cuvettes (950 μL of PBS pH 8.5 + 50 μL sample). To calculate the progress of the reaction, the absorbance of the control solution was subtracted from the absorbance of the sample. Reaction kinetics measurement was performed once for each manufacturer's peptide.

The amount of thiol groups of the col IV-SH was quantified using the molar absorptivity of Ellman's reagent. 4 mg $mL^{-1}$ solution of Ellman's reagent was prepared in reaction buffer (0.1 M PBS, pH 8.0, containing 1 mM EDTA). Two tubes were prepared with 1.25 mL of reaction buffer and 25 μL of the Ellman's reagent, and added with 125 μL of either the col IV-SH sample or pure reaction buffer, which served as the blank.

After 15 min, the absorbance of the sample was measured at 412 nm against the blank using the UV/VIS spectrophotometer. The concentration of thiol groups was calculated based on the molar extinction coefficient of Ellman's reagent (14 150 $M^{-1}cm^{-1}$) and Equation (4)

$$c = \frac{A}{bE} \quad (4)$$

where $A$ is the absorbance of the sample at 412 nm, $b$ is the length of the light path (1 cm), and E is the molar extinction coefficient.

### 2.8. Cell culture and in vitro analysis

All cell studies were conducted with approval from the Ethics Committee of the Pirkanmaa Hospital District (Tampere, Finland) under the approval number R15161 for use of adipose stem cells in research and approval number R05116 to derive, culture, and differentiate hESC lines for research. The hASCs were isolated from adipose tissue samples from a female donor during elective plastic surgery at Tampere University Hospital (Tampere, Finland) under patient's written consent, as described previously [36,37]. The flow cytometric cell characterization profile of the hASCs used in this study is described elsewhere [20]. The hASCs were cultured in a medium containing DMEM/F-12 supplemented with 5% human serum, 1% GlutaMAX™ and 1% antibiotics. The cells were maintained in T175 cell culture flasks at 37 °C in 5% $CO_2$, and passaged using TrypLE™ Select. Cells were maintained up to passage 4 prior to encapsulation in hydrogels. For encapsulation, hASCs were detached from cell culture flasks, collected by centrifugation and counted. The required number of cells for each hydrogel was collected in Eppendorf tubes, and the cells were pelleted. Supernatant was removed and cell pellets were mixed by thorough pipetting into the hydrazide component (HA-CDH or HA-DA-CHD) at a concentration of $2 \times 10^6$ cells $mL^{-1}$. The hydrogels were then formed by mixing the cell-containing hydrazide component with an equal volume of HA-Ald in either 24-well cell culture inserts (Merck Millipore), total volume of 100 µL, or custom-made polydimethylsiloxane (PDMS) molds with 10 mm diameter wells, total volume of 200 µL. The hydrogels were allowed to gel for 2 h in a humid atmosphere at RT before adding medium. The cell-laden hydrogels were then cultured either in hASC medium (for 3D cell survival determination) or CnT-Prime-CC (for co-culture of hASCs and hESC-LESCs) at 37 °C in 5% $CO_2$. To create the compartmentalized stem cell implants, the hASCs were cultured alone for 24 h before conjugation of col IV-SH and seeding of hESC-LESCs.

The hESC-LESCs were differentiated from human embryonic stem cell line Regea08/017 cultured in feeder-free conditions, according to our previously published protocols [38,39]. The hESC-LESCs were thawed from cryostorage to the basement membrane protein-conjugated hydrogels in a concentration of $0.9–1.5 \times 10^6$ cells $cm^{-2}$, with further culture of the cell-laden hydrogel in CnT-30 medium containing 0.5% antibiotics. For surface attachment study, hESC-LESCs were cultured on the hydrogels for seven days. The hydrogel scaffolds containing both hASCs and hESC-LESCs were cultured in CnT-30 medium for two to five days before transplantation in the porcine organ culture model or fixation for histological evaluation.

The viability of hESC-LESCs on the surface-modified hydrogels was evaluated based on cell morphology, with light microscope images taken with Zeiss Axio Vert A1 (Carl Zeiss AG, Jena, Germany), and compared quantitatively using PrestoBlue® reagent. For PrestoBlue® analysis of cell metabolism, three parallel samples were analyzed for each condition. The samples were washed once with DPBS, and the PrestoBlue® reagent, diluted 1:10 (v/v) in CnT-30 medium, was added to the samples. The samples were incubated for 30 min at 37 °C, after which 2 × 100 µL samples of the medium were collected on a 96-well plate. The fluorescence values for the medium samples were measured using Viktor 1420 Multilabel Counter (Wallac, Turku, Finland) at 544 nm excitation and 590 emission wavelengths.

For hASCs encapsulated into the hydrogels, viability was evaluated qualitatively using LIVE/DEAD® viability/cytotoxicity kit, and quantitatively with CyQUANT cell proliferation kit and PrestoBlue® after 1, 3, 7 and 10 days. For Live/Dead staining, the hydrogels were removed from their molds, washed with DPBS and incubated with Live/Dead staining solution containing 2 µM Calcein AM and 1 µM Ethidium homodimer diluted in DPBS in 37 °C for 30–45 min. The samples were washed once, and imaged using Olympus IX51 fluorescence microscope equipped with a DP71 camera (Olympus Corporation, Tokyo, Japan). For CyQUANT analysis of hydrogel DNA content, three gels with hASCs and one blank gel were collected in each time point to 2 mL Eppendorf tubes and frozen in −80 °C. After thawing, 100 µL of the CyQUANT lysis buffer was added to the samples, which were then mechanically homogenized using an Ultra-Turrax disperser (IKA Labortechnik, Staufen, Germany). Samples were centrifuged at 8000 g for 30 s to remove any remaining hydrogel, with the final sample diluted 1:10 in CyQUANT lysis buffer. The diluted samples were then pipetted to 96-well plates with CyQUANT Dye, and the fluorescence was read at 480/520 nm with Victor 1420 Multilabel Counter microplate reader. For cell number quantitation, the measured fluorescence values were compared to a reference standard curve created from 2D cultured hASCs. PrestoBlue® analysis from encapsulated hASCs was conducted as described previously in Ref. [20]. Statistical testing of the cell viability results was performed by two-way ANOVA between HA-DOPA and HA-HA gels using GraphPad Prism v5.02.

### 2.9. Porcine corneal organ culture

Porcine eyes were obtained from a local abattoir. The eyes were kept in cold DPBS containing 2% antibiotics for up to 4 h before dissection and transfer to the organ culture. The eyes were processed as previously described, and cultured partially submerged in CnT-Prime-CC medium with 1% antibiotics and 0.1% amphotericin B [20]. Prior to implantation of the cell-laden hydrogels, an epithelium defect was induced by applying a circular Whatman paper impregnated with 1 M NaOH on the cornea surface for 40 s, followed by rinsing with DPBS and epithelial scraping. For hydrogel implantation, the organ-cultured corneas were immobilized on a Barron artificial anterior chamber (Katena products Inc., Denville, NJ, USA), where a partial depth incision was made to the stroma using a 5-mm trephine, from which the stromal button was excised. The hydrogel implant containing hASCs and hESC-LESCs was cut to size using a 5-mm trephine, and the implant was transferred to the stromal wound using a flat spatula. After hydrogel implantation, the corneas were transferred to 6-well plates, covered with soft contact lenses and cultured for additional seven days in CnT-30 medium at 37 °C, 5% $CO_2$.

To determine the differentiation potential of implanted hASCs in the corneal organ culture, 50 µL HA-HA and HA-DOPA gels with encapsulated hASCs (300 000 cells/gel) were made directly into the stromal wounds, with four replicates of each gel. The corneas were cultured for 10 days in keratocyte differentiation medium (KDM) containing Advanced DMEM supplemented with 10 ng $mL^{-1}$ basic fibroblast growth factor (bFGF), 0.1 mM ascorbic acid-2-phosphate and 1 µM retinoic acid, as described previously in Refs. [11,40]. The gels with cells were collected from the corneal wounds after the culture period into TRIreagent, and the samples were homogenized using Bioruptor sonicator (Diagenode SA, Belgium) (30 s ON, 30 s OFF, 2 cycles). RNA from the samples was isolated by adding chloroform to the TRIreagent solution, vortexing and centrifugation (12 000 g for 10 min). The upper chloroform phase was collected to a new tube and isopropanol was added, followed by vortex and centrifugation (12 000 g, 10 min). The supernatant was removed, and the RNA pellet was eluted into 70% ethanol, vortexed and centrifuged (12 000 g, 10 min). The supernatant was removed and remaining pellet was air-dried and eluted into 30 µl RNAse free water. The amount of RNA was quantitated using NanoDrop spectrophotometer (Thermo Fisher Scientific). Enough RNA to perform

qRT-PCR was obtained from three replicates for both gels, and the RNA was treated with DNAse I and transcribed to cDNA using High capacity cDNA reverse transcription kit (Applied Biosystems, Thermo Fisher Scientific). As a control, 2D differentiation of hASCs was performed on standard tissue culture plastic 6-well plates, culturing them in KDM for 10 days. Control samples of undifferentiated hASCs and 2D differentiation were collected for quantitative real-time polymerase chain reaction (qRT-PCR) with Qiagen RNeasy Mini Kit according to manufacturer's instructions, and transcribed to cDNA together with RNA from the gel samples. qRT-PCR analysis for three corneal keratocyte markers, keratocan (KERA), lumican (LUM) and aldehyde dehydrogenase 3A1 (ALDH3A1) was run with Applied Biosystems real time PCR instrument. The relative fold change of gene expression was analyzed using the $2^{-\Delta\Delta Ct}$ method.

### 2.10. Histological analysis and immunofluorescence

For histological analysis, the porcine organ culture corneas were fixed using 4% paraformaldehyde (PFA) for 3 h at RT, submerged in Tissue-Tek OCT (Sakura Finetek Europe) at 4 °C overnight, and snap-frozen in liquid nitrogen. 8 mm thick sections were cut from the samples and air dried for 1 h at RT. Cell-laden hydrogel samples were similarly processed, with 30 min fixation in 4% PFA. Sections from the porcine corneas were then immunohistochemically stained against human cell surface marker TRA-1-85 to detect implanted human cells. 2.5% normal horse serum (Vector ImmPress reagent, Vector Laboratories Inc.) was used to block unspecific binding. Samples were then labeled overnight at 4 °C with primary mouse IgG antibody TRA-1-85 (courtesy of Peter Andrews, University of Sheffield) diluted 1:100 (v/v) in 0.5% bovine serum albumin (BSA). Intrinsic peroxide activity was blocked by incubating the samples with 3% $H_2O_2$ for 10 min at RT, followed by labelling with Vector ImmPress horse anti-mouse IgG (containing horseradish peroxidase) for 30 min at RT. The antibody labelling was visualized by peroxidation reaction using DAB + chromogen system (Dako North America, Inc., Carpinteria, CA, USA), which was performed for 30 s at RT. The tissue was counterstained using Mayer's hematoxylin, followed by dehydration, and mounting using Coverquick mounting medium (VWR, Helsinki, Finland). Samples were imaged using Hamamatsu NanoZoomer S60 (Hamamatsu Photonics Norden, Kista, Sweden) whole slide scanner, and images were obtained using NDP.view2 viewing software.

Immunofluorescence staining, for hESC-LESCs on top of hydrogels and the transverse cryosections of the cell-laden hydrogels, was carried out using primary antibodies against p63α, p40, cytokeratin 12 (CK12), and col IV. Details of the antibodies are listed in Table 1. The hydrogel samples on well plates were fixed with 4% PFA for 30 min at RT, followed by washing with DPBS. The samples were then permeabilized using 0.1% Triton X-100 for 15 min, followed by blocking with 3% BSA and incubation with primary antibodies diluted in 1% BSA overnight at 4 °C. After washing with DPBS, the samples were incubated with fluorescently labeled secondary antibodies (Table 1) diluted in 1% BSA, for 1 h at RT. The samples were then washed and mounted under coverslips using mounting medium containing 4′,6-Diamidino-2-Phenylindole (DAPI) (Vectashield® from Vector Laboratories or ProLong™ Gold from Thermo Fisher Scientific) and imaged using Olympus IX51 fluorescence microscope. Fluorescent images were converted to color images and adjusted for contrast and brightness using Photoshop.

## 3. Results and discussion

### 3.1. Synthesis and characterization of dopamine-functionalized HA hydrogel

We have previously developed hydrazone-based robust hydrogels using HA-aldehyde (HA-Ald) and HA-carbodihydrazide (HA-CDH) with exceptional enzymatic stability and swelling characteristics [19]. We used this two-component biorthogonal system for fabricating the compartmentalized cellular scaffold for corneal applications. In order to introduce the tissue adhesive properties to facilitate sutureless implantation of the scaffold, we conjugated L-dopamine moiety in the polymer. The degree of dopamine functionalization was 14%, as determined by $^1$H NMR (Fig. S1 in Supplementary Information). The aldehyde and CDH groups were grafted on HA following our previously optimized carbodiimide protocol [19] and the percentage of aldehyde and CDH functionalization was around 10% (with respect to the disaccharide repeat units), which was quantified by $^1$H NMR (Fig. S2 in Supporting Information) and UV/VIS spectroscopy. We utilized HA gels with similar aldehyde and CDH modification without dopamine units as the control group. The dopamine-functionalized HA-gels were designated as HA-DOPA, while the control gel was designated as HA-HA. Their structures are presented in Fig. 1.

### 3.2. HA-HA and HA-DOPA gels display highly elastic character

We performed rheological evaluation to estimate the viscoelastic properties of HA-HA and HA-DOPA gels by measuring the gel deformation following the frequency sweep method. The gels were subjected to strain sweep to determine the linear viscoelastic region (LVR) of the hydrogel, followed by a frequency sweep test at 0.1–10 Hz using a constant strain within the LVR (Fig. 2a). The gels showed storage moduli ($G'$) of 898.81 ± 16.46 Pa and 619.57 ± 13.02 Pa and loss moduli ($G''$) of 3.046 ± 0.07 Pa and 1.88 ± 0.624 Pa respectively for HA-HA and HA-DOPA gels. The storage modulus $G'$ was consistently higher than the loss modulus $G''$ throughout the screened frequency range suggesting that both the hydrogels were stable and possessed viscoelastic properties. The tan δ, which represents the ratio of storage and loss moduli, was found to be significantly less than 1 (0.0034 and 0.0030 for HA-HA and HA-DOPA gels respectively) suggesting a highly elastic character for these gels. By using the modulus data, we estimated the average mesh size ξ (representing the distance between the entanglement points or probable pore size) and the average molecular weight between the crosslinks $M_c$ by using the rubber elastic theory that can be applied to highly elastic hydrogels [41]. These calculations revealed that average mesh size ξ was 16.6 nm and 18.8 nm while the $M_c$ was 41.46 kg mol$^{-1}$ and 56.96 kg mol$^{-1}$ for HA-HA and HA-DOPA gels respectively. Thus, HA-HA gel was stiffer and more compact than the HA-DOPA gel, with smaller ξ and $M_c$.

Next, we investigated the effect of encapsulated stem cells on the

**Table 1**
Antibodies used for immunofluorescence staining.

| Antibody | Host | Supplier | catalog no. | dilution [v/v] |
|---|---|---|---|---|
| p63α | rabbit | Cell Signaling Technology | 4892 | 1:200 |
| p40 | mouse | Biocare Medical | 3066 | 1:100 |
| CK12 | goat | Santa Cruz Biotechnology | sc-17099 | 1:200 |
| collagen IV | goat | Millipore | AB769 | 1:200 |
| anti-rabbit Alexa-488 | donkey | Molecular Probes | A21206 | 1:800 |
| anti-goat Alexa-568 | donkey | Molecular Probes | A11057 | 1:800 |
| anti-mouse Alexa-647 | donkey | Molecular Probes | A31571 | 1:800 |

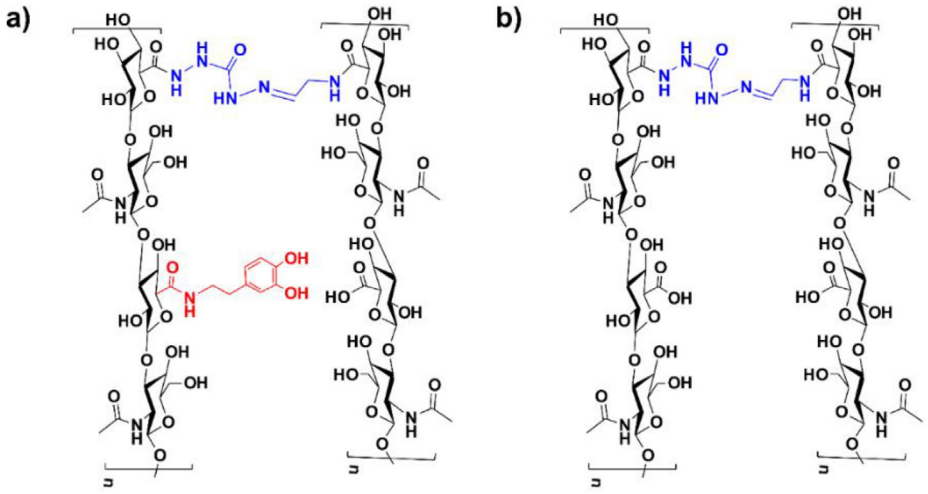


**Fig. 1.** Chemical structures of hydrazone-crosslinked HA-DOPA (a) and HA-HA (b) hydrogels.

viscoelastic properties of the scaffold (Fig. 2b). We cultured hASCs in HA-HA and HA-DOPA gels ($2 \times 10^6$ cells $mL^{-1}$) for 24 h as described in section 2.8. After that, the cell-laden hydrogels were extracted from their molds and we performed the rheological measurements as described in section 2.3. We found that the encapsulation of cells within the hydrogel resulted in the reduction of storage modulus ($G'$) for both HA-HA and HA-DOPA gels. This could be attributed to two factors, the presence of different serum proteins and biomolecules in the cell culture medium and the cell surface proteins. The gels showed storage moduli $G'$ of 309.15 ± 5.63 Pa and 483.70 ± 7.35 Pa and loss moduli $G''$ of 6.94 ± 1.71 Pa and 11.00 ± 1.69 Pa respectively for HA-HA and HA-DOPA gels at the frequency of 1 Hz. Interestingly, when we compare the two gels formulated in PBS to the gels formulated with cells in cell culture medium we observed that the change in $G'$ was smaller in

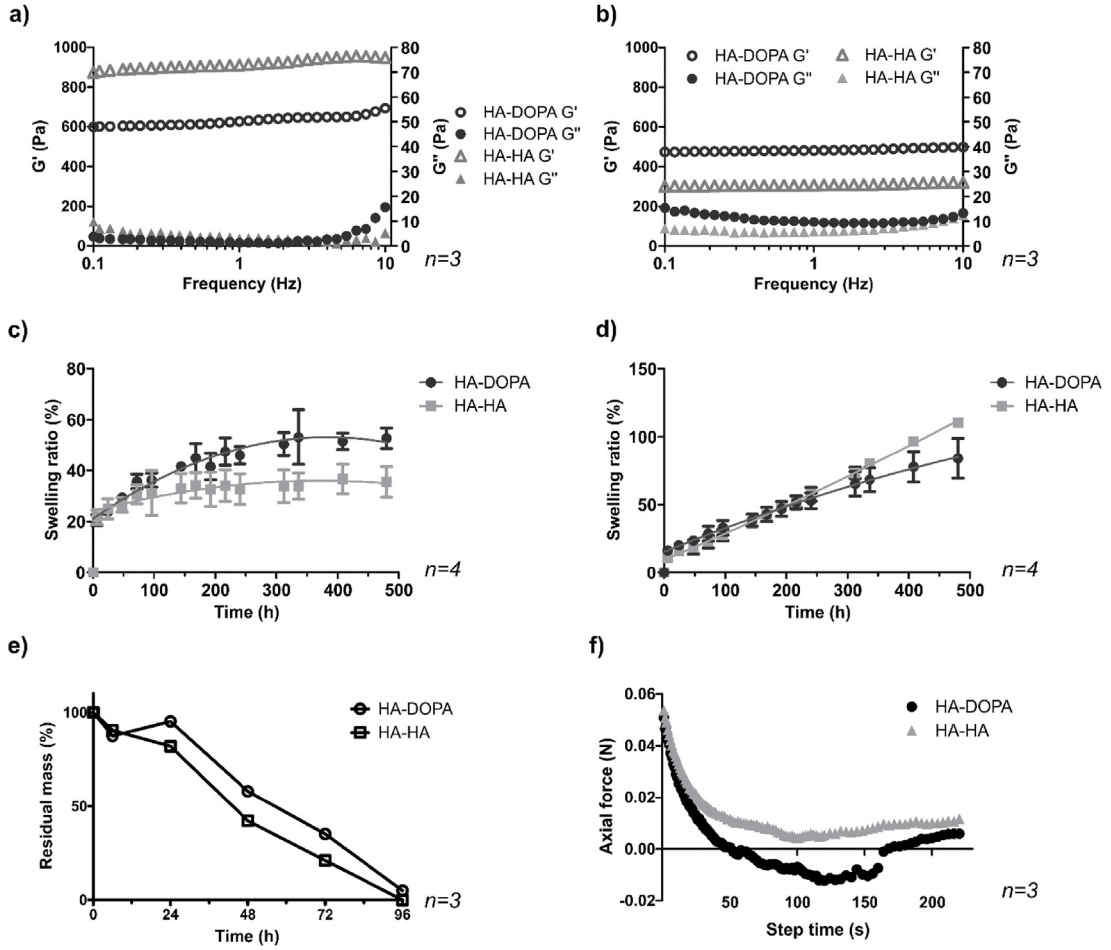


**Fig. 2.** Material characterization of HA-DOPA and HA-HA gels. a) Rheological measurement of $G'$ and $G''$ in the frequency sweep mode. b) Frequency sweep of $G'$ and $G''$ of hydrogels with encapsulated hASCs. c) Hydrogel swelling ratios in PBS. d) Hydrogel swelling ratios in cell culture medium. e) Enzymatic degradation of the hydrogels in the presence of hyaluronidase. f) Adhesion force measurement of the hydrogels to corneal surface.

**Table 2**
Material properties of HA-DOPA and HA-HA gels.

| Hydrogel | n | $G'$ [Pa] | G″[Pa] | tan δ[G′/G″] | $\xi$ [nm] | $M_C$ [kg mol$^{-1}$] |
|---|---|---|---|---|---|---|
| HA-HA | 3 | 898.81 ± 16.46 | 3.046 ± 0.07 | 0.0034 | 16.6 | 41.46 |
| HA-DOPA | 3 | 619.57 ± 13.02 | 1.88 ± 0.624 | 0.0030 | 18.8 | 56.96 |
| HA-HA with cells | 3 | 309.15 ± 5.63 | 6.94 ± 1.71 | 0.0224 | 23.7 | 123.27 |
| HA-DOPA with cells | 3 | 483.70 ± 7.35 | 11.00 ± 1.69 | 0.0227 | 20.41 | 79.38 |

HA-DOPA gels when compared to HA-HA gels. The $G'$ decreased with the incorporation of cells in HA-HA gels from 898.81 ± 16.46 Pa to 309.15 ± 5.63 Pa, and in HA-DOPA from 619.57 ± 13.02 Pa to 483.70 ± 7.35 Pa. This observation indicates that the dopamine units form some kind of interpenetrating network or exert adhesive forces that prevent the swelling and disruption of molecular crosslinks. This is further evidenced by the average mesh size ξ values for both gels. In the presence of cells, HA-DOPA and HA-HA had average mesh size 20.41 nm and 23.7 nm respectively, while without cells the values were 18.8 nm and 16.6 nm, respectively. This means that the HA-DOPA gel had a larger pore size in PBS, whereas in the presence of cells, the average mesh size was reduced, presumably due to adhesive forces exerted by the dopamine moiety. The tan δ was found to be less than 1 (0.0224 and 0.0227 for HA-HA and HA-DOPA gels respectively) suggesting elastic characteristics for these gels, but the degree of elasticity was much lower in the presence of cells compared to the gels without encapsulated cells (tan δ 0.0034 and 0.0030 for HA-HA and HA-DOPA gels respectively). Thus, in the presence of cells, HA-DOPA gels were stiffer and more compact with smaller $\xi$ and $M_c$ than HA-HA gels. The material characteristics are summarized in Table 2.

For the cornea, the material property most often described is the shear modulus. The shear modulus of the native cornea varies with depth, with the anterior stroma having a higher modulus (7.71 kPa) than the deeper parts of the cornea (1.31–1.99 kPa) [42]. Although our application focuses on replacing the anterior stromal part of the cornea with the hydrogel scaffold, we consider the mismatch of the initial mechanical properties of the material to the cornea to be inconsequential for the final regenerative target. For stable corneal regeneration and integration, the stromal cells should secrete their own extracellular matrix (ECM) and remodel their environment. This has been previously shown during a 4-year follow-up of cell-free stromal implants composed of densely crosslinked collagen hydrogels, where surrounding stromal cells were seen to slowly replace the implant with stromal tissue [43]. Our approach aims at faster remodeling and integration of the scaffold to the corneal tissue through encapsulation of hASCs.

### 3.3. HA-DOPA gel shows good swelling stability in physiological conditions

To evaluate the swelling property of the HA-HA and HA-DOPA gels, we measured their weight increase in phosphate buffered saline (PBS, pH 7.4) and cell culture medium at 37 °C (Fig. 2c and d). Both gels showed similar swelling behavior, but the swelling kinetics differed in PBS compared to cell culture medium. In PBS, the hydrogels reached an equilibrium swelling state after 1 week, whereas in medium, the hydrogels continued to swell in a linear manner throughout the measurement period. In PBS, both gels displayed an initial 20% burst in swelling upon hydration, after which the swelling slowed down and subsequently leveled at approximately 34% for HA-HA and 50% for HA-DOPA during three weeks. The higher swelling ratio of HA-DOPA gel may be associated with the larger average mesh size, which allows more water permeability inside the hydrogel network. Interestingly, in medium, the swelling ratio for HA-HA surpassed that of HA-DOPA after the 1-week time point, ultimately reaching 110% for HA-HA and 85% for HA-DOPA in three weeks. We believe the sustained swelling properties of the two hydrogels in cell culture medium are attributed to the dynamic nature of the hydrazone bond, which may undergo exchange with proteins present in the medium. Lower swelling in medium observed for HA-DOPA may indicate that the hydrazone bond dynamics are complemented by additional interpenetrating crosslinks introduced by dopamine self-polymerization or adhesive forces exerted by dopamine, which was supported by a slight increase in intensity of the slight brown hue of HA-DOPA gels during prolonged exposure to cell culture medium, as discussed in detail in Section 3.5.

Hydrazone crosslinking using CDH-derived hydrazones has been shown to be considerably more stable than hydrazone crosslinks from other hydrazides, due to the resonance stabilization effect across the hydrazone bond [19]. The engraftment of dopamine residues to HA increased the PBS swelling capacity of the gels, indicating that the incorporation of dopamine slightly hindered the crosslinking efficacy of the gels. Conversely, the HA-DOPA gels were more stable in medium, which arguably resembles the *in vivo* environment more closely than PBS, indicating their overall suitability for tissue engineering applications. However, in the cornea, the tissue environment is not as dilute as the conditions of the swelling study. *In vivo*, the hydration of corneal tissue is maintained by the pumping mechanism of the endothelium, and the surface of the cornea is wetted by tear fluid secreted by the lacrimal and Meibomian glands and the goblet cells of the conjunctiva, with its varying composition of lipids, proteins and small molecules [44]. The actual swelling of the implants in the intended application should hence be studied in a more tissue-specific environment.

We studied the *in vitro* degradation kinetics of the hydrogels in the presence of hyaluronidase (HAse), a ubiquitous enzyme known for the *in vivo* degradation of HA. At a concentration of 20–50 U mL$^{-1}$ of HAse, both HA-HA and HA-DOPA gels displayed complete digestion in 96 h (Fig. 2e). Although, the concentration of HAse used in this experiment is not directly comparable to that in the eye, the enzymatic degradation of the scaffold implies that the chemical modifications on the HA-HA and HA-DOPA gels did not disrupt the native bioactivity and the biodegradability of the polymer. For final applications, the rate of degradation *in vivo* should be studied further to match the regeneration of the replaced corneal tissue, which can take from months to even years to complete [45].

### 3.4. HA-DOPA adheres strongly to the corneal surface

Adhesion of biomaterial scaffold to the defect site is of paramount importance for successful tissue regeneration. Scaffolds bearing aldehyde functional groups are known to display tissue adhesive properties [46]. However, as the aldehyde functional groups are utilized for hydrazone crosslinking, the free aldehyde residues are not sufficient enough to provide the adhesiveness required for scaffold integration. We anticipated that incorporation of dopamine groups would further augment the adhesive properties of the scaffold. We conjugated 14.4% dopamine units on the HA backbone, as the overall HA modification (hydrazide and dopamine moiety) must not exceed 25% [47] in order to preserve the biodegradability and activity of the biopolymer.

We performed a rheometric tack adhesion test to quantify the adhesion properties of HA-HA gels and HA-DOPA gels with the corneal surface. Although both HA-HA and HA-DOPA gels displayed some adhesion properties, HA-DOPA clearly showed greater adhesion to the cornea with cohesive failure between the probe and the gel. This can be

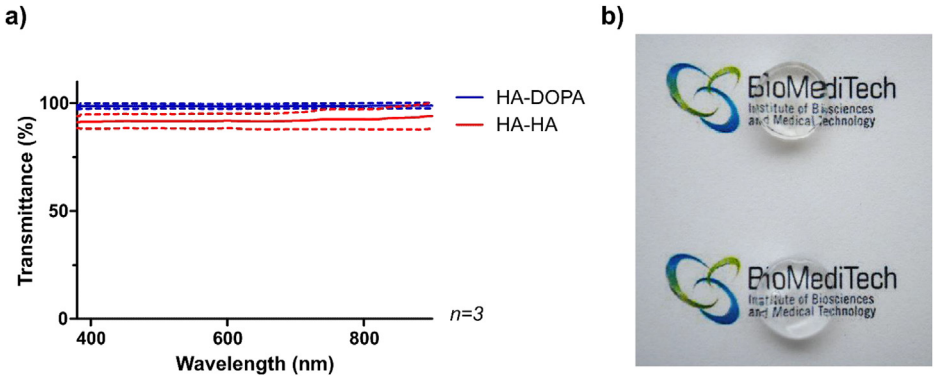


**Fig. 3.** Transmittance and transparency HA-DOPA and HA-HA gels. a) Transmittance of light at different wavelengths through the hydrogels. b) Transparency of the hydrogels illustrated by photography of HA-DOPA (upper) and HA-HA (lower) gels on text.

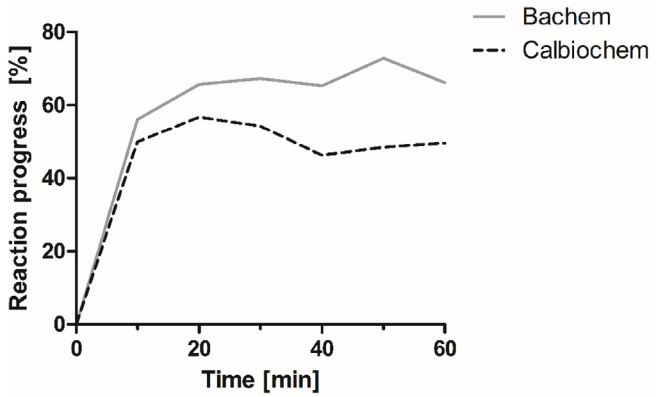


**Fig. 4.** Reaction kinetics measurement of surface conjugation of Cys-terminated laminin-derived peptide. The reaction progress was calculated based on the presence of free thiol groups in the reaction solution at different time points.

seen from Fig. 2f, as more negative force was required to separate the probe and the gel surface.

### 3.5. Hydrogels display excellent transparency for corneal applications

Transparency is a key property of any biomaterial used for corneal applications. The native cornea exhibits light transmission of 90–95% in wavelengths ranging from 600 to 1000 nm [48]. To analyze the transparency of the hydrogels, we measured the transmittance of light over the visible light spectrum (380–900 nm), shown in Fig. 3a. Both hydrogels showed over 90% light transmittance over the whole visible spectrum. Interestingly, transmittance values for HA-DOPA (98 ± 2.39%) measured even higher than for HA-HA (95 ± 4.64%). This indicates that the slight brown hue caused by the DOPA residues, seen in Fig. 3b, did not seem to hinder the transmittance of light through the HA-DOPA gel, whereas the lower transmittance of HA-HA might be caused by minute inhomogeneity of the gel occurring through mixing of the sucrose-dissolved HA-CDH component and HA-Ald dissolved in PBS.

The brown coloration is a distinct trait of dopamine-containing materials. As dopamine residues self-polymerize, they display an intense brown color [49]. Dopamine-functionalized hydrogels reported so far generally rely on self-polymerization reaction or metal-coordination for effective crosslinking [28–31]. However, in our hydrogel implants, the dopamine residues are not responsible for the crosslinking, leaving them free to participate in the surface modification and tissue-adhesion of the preformed hydrogel implant. This results in a transparent hydrogel, which is suitable for corneal applications. Further *in vivo* studies are warranted to assess the impact of dopamine functionalization and transparency on the regenerated corneal tissue.

### 3.6. Immobilization of cell adhesive factors enables cellular compartmentalization in tissue adhesive hydrogels

One major limitation of HA-based hydrogels for 3D cell culture is the poor cell adhesion due to the lack of binding sites for integrins, the major mediators of cell adhesion to the ECM. However, the encapsulated cells can probe their microenvironment and secrete ECM making it conducive for cell growth and differentiation [50,51]. To achieve cellular compartmentalization of the two stem cell populations, we conjugated cell adhesive peptides and proteins on the surface, exploiting the Michael acceptor characteristics of the dopamine residue. Our first choice of cell adhesive molecule was a cysteine-terminated laminin-derived synthetic peptide (CDPGYIGSR) which could be covalently grafted to the surface of the hASC-encapsulated hydrogel. This laminin-derived peptide contains the cell adhesion motif YIGSR, which has been previously shown to have significant potential for improving primary corneal epithelial cell adhesion to biomaterial surfaces [52]. Furthermore, recombinant laminin is an integral component of the culture substrate for the differentiation and culture of hESC-LESCs [38]. Ellman's quantitation of free thiols (Fig. 4) revealed that the conjugation reaction initially progressed rapidly, and reached a plateau after 10–20 min. Comparison of the same peptide from different manufacturers produced similar reaction kinetics, while the Bachem peptide conjugation reaction progressed further until approximately 70% of the peptide were bound to the surface, and was thus selected for the cell attachment study. Although we could achieve excellent conjugation of the laminin peptide on to the preformed hydrogels by Michael addition reaction, we could obtain only sparsely distributed hESC-LESCs on these peptide-modified surfaces (Fig. 5h). Subsequently, another component of hESC-LESC culture substrate, human collagen type IV (col IV) was chosen as the preferential basement membrane protein. Col IV was thiolated using 2-iminothiolane (Traut's reagent) to col IV-SH with the necessary reactive groups for Michael addition. The conversion of primary amines in col IV to thiol groups, as determined by Ellman quantitation assay, was found to be 57 ± 4.2% in this study.

The hESC-LESCs cultured on col IV-SH conjugated HA-DOPA surfaces displayed efficient cell adhesion and better long-term cell viability than on similarly treated HA-HA (Fig. 5). Interestingly, we observed some degree of hESC-LESCs attachment even when unmodified col IV was coated on the HA-DOPA gels (Fig. 5e-g) indicating the adhesive tendency of dopamine-functionalized surfaces. Also the HA-HA control gel also displayed some binding of col IV-SH (Fig. 5i-k). This may be attributed to the dynamic nature of the hydrazone bond, allowing the thiol-containing peptides or proteins to undergo thiazolidine crosslinking with aldehyde groups available on the scaffolds [53]. The microscopic evaluation of cell morphology was supported by the PrestoBlue® cell viability measurement (Fig. 5q-r), which shows that initially the hESC-LESCs attach on both gel types, but there is a gradual

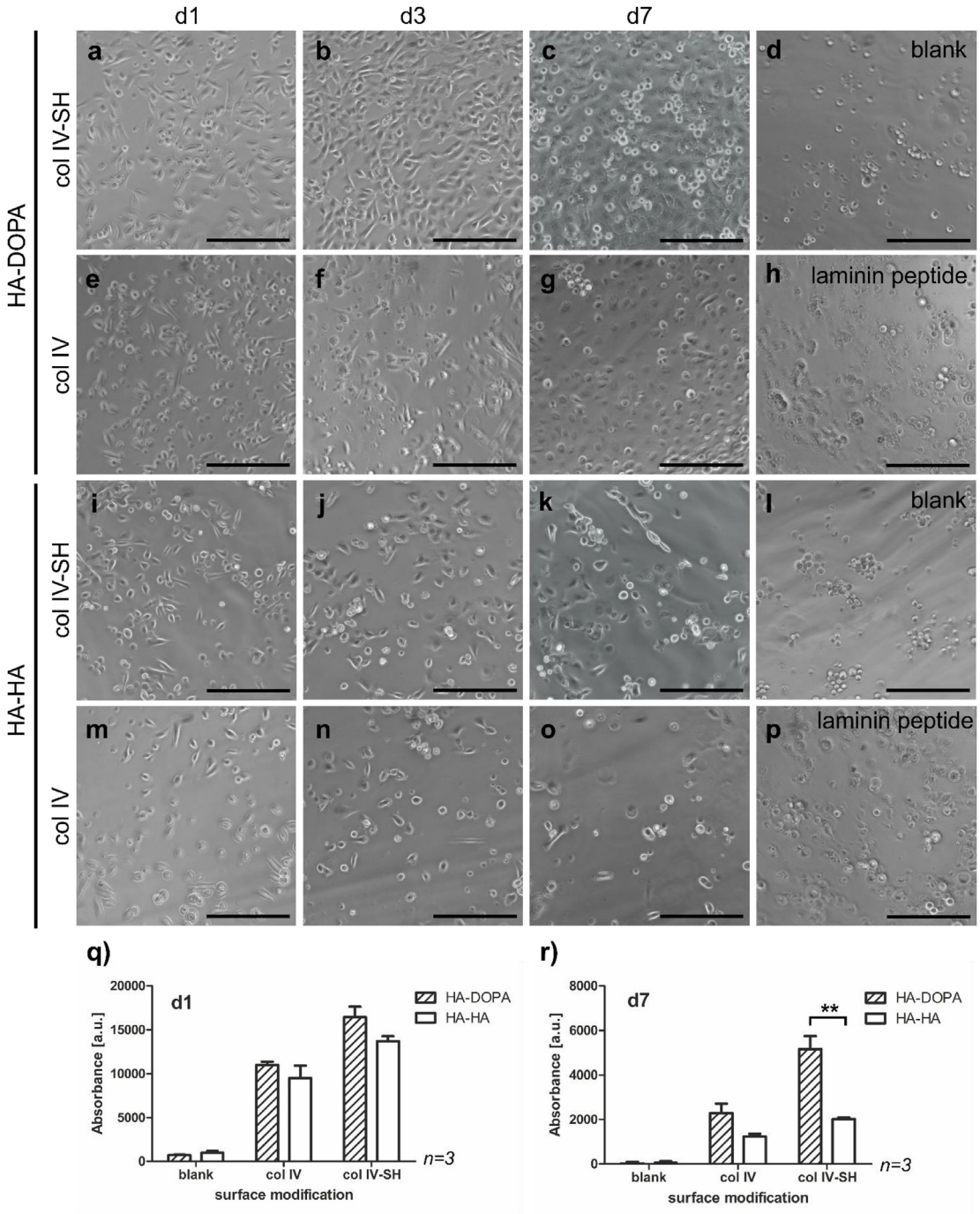


**Fig. 5.** Morphology and viability of hESC-LESCs on surface-modified hydrogels. a-c) hESC-LESCs seeded on thiolated col IV (col IV-SH)-immobilized HA-DOPA after 1 day, 3 days and 7 days of culture, respectively. The same time points are also shown for HA-DOPA with non-thiolated col IV (e–g) and col IV-SH on HA-HA (i–k) and non-thiolated col IV on HA-HA (m–o). Images d) and l) represent hESC-LESC morphology observed on unmodified HA-DOPA and HA-HA surfaces, respectively. Images h) and p) are representative images of hESC-LESCs 2 days after plating on laminin-derived peptide –immobilized HA-DOPA and HA-HA, respectively. Graphs q) and r) show the PrestoBlue® viability measurements of hESC-LESCs on col IV –modified hydrogel surfaces at day 1 and day 7, respectively. Scale bars in images are 200 μm ** denotes statistical significance at $p < 0.01$.

loss of cells from the HA-HA gels, resulting in a significantly higher cell viability on HA-DOPA at day 7. The immunofluorescence staining for col IV in hydrogel cross-sections, shown in Fig. 6a, verified the presence of high amounts of col IV on the col IV-SH-conjugated HA-DOPA, but only very little on HA-HA at 2 days after conjugation.

The cells grown on the HA-DOPA gels for 7 days showed appropriate protein expression for progenitor-type hESC-LESCs, as shown in Fig. 6b. The continued expression of the limbal stem cell marker ΔNp63α, which was confirmed by the co-labelling of p63α and p40 in cell nuclei, together with the low expression levels of epithelial maturation marker cytokeratin 12 (CK12) indicated that the hESC-LESCs retained their progenitor-like phenotype after 1 week of culture on these substrates. The hESC-LESCs still present on col IV-SH-conjugated HA-HA gels after 7 days also retained similar marker expression, although the portion of ΔNp63α-positive cells was smaller than on HA-DOPA. This suggests that covalent conjugation of the protein is indispensable on the hydrogel surface for the continued growth and maintenance of hESC-LESCs.

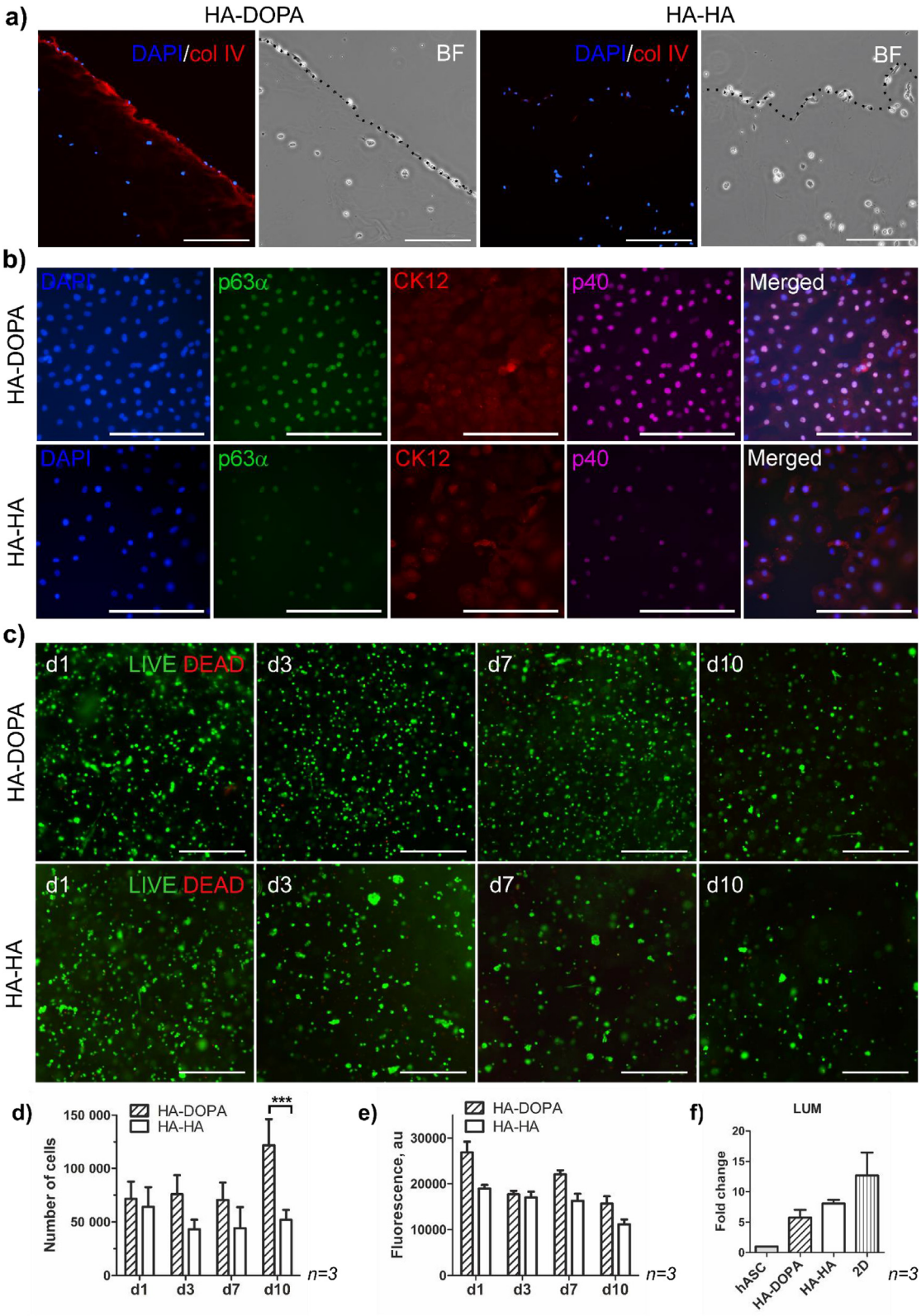


**Fig. 6.** Covalent surface conjugation of col IV-SH enables the existence of two distinctly organized human stem cell types in the hydrogels. a) Fluorescent staining of col IV at the surface of HA-DOPA and HA-HA gels 2 days after conjugation, the dotted line represents the surface of the hydrogel. b) hESC-LESCs cultured on col IV-SH-conjugated HA-DOPA and HA-HA for 7 days express the limbal stem cell markers p63α and p40, with low expression of epithelial differentiation marker CK12. c) Live/Dead staining of hASCs inside hydrogels at different time points, live cells are shown in green, and dead cells in red. d) CyQUANT results representing the number of hASCs in the gels during culture. e) PrestoBlue® quantitation metabolic activity of hASCs inside gels during culture. f) Relative gene expression of hASCs 10 days after implantation to *ex vivo* corneal model and 2D control condition showed increased expression of lumican, an extracellular matrix component of the cornea. Values reflect fold changes in mRNA expression over undifferentiated hASCs. Scale bars in images a) and b) are 200 μm, in c) 500 μm *** denotes statistical significance at $p < 0.001$. (For interpretation of the references to color in this figure legend, the reader is referred to the Web version of this article.)

The encapsulated hASCs remained viable within the HA-DOPA and HA-HA gels for 2 weeks of culture, as presented in Fig. 6c. The Live/Dead staining shows only few dead cells, whereas the amount of live cells remains high throughout the culture period, with slightly more cells in the HA-DOPA gels than the HA-HA. Furthermore, within the HA-DOPA gels hASCs occurred mostly as single cells or small groups of cells with some apparent elongation, whereas in HA-HA more rounded cell clustering was observed. This observation is interesting as HA gels lack integrin binding sites and the cells cultured in these gels traditionally show rounded morphology. We hypothesize that the adhesive nature of the DOPA residues in HA-DOPA gels may promote entrapment of the endogenous ECM produced by the cells, thus promoting cell elongation within these gels. In accordance with our results, mesenchymal stem cells within hydrogels have been shown to produce very rapidly a cell-type specific ECM around themselves, through which they interact with the surrounding hydrogel [51].

The CyQUANT results, shown in Fig. 6d, for assessing the number of cells within the HA-DOPA and HA-HA gels also indicate higher hASC viability and proliferation within the HA-DOPA gels than in HA-HA in all time points, with significantly higher number of cells on day 10. However, the PrestoBlue® results (Fig. 6e) of cells' metabolic activity within the gels show less pronounced difference between the groups. Overall, the HA-DOPA gels were superior to HA-HA gels in terms of cell growth of both hESC-LESCs and hASCs.

### 3.7. HA-DOPA gels support sutureless implantation in porcine corneal organ culture

As a proof-of-concept in using the tissue adhesive hydrogel implants for delivering epithelial and stromal regenerating cells to the cornea, we performed an anterior lamellar keratoplasty procedure (i.e. removal of part of the outer stroma) in an *ex vivo* cornea organ culture model with excised porcine corneas. We transplanted the approximately 2 mm thick hydrogel implants into the created stromal wounds, without utilizing additional means of securing the implants in place. Due to the fitted trephination of both the wound and the implant, as well as the static nature of the subsequent organ culture, all implants remained in place for the duration of the culture. However, during manipulation of the corneas for fixation and histology, some HA-HA implants were extruded from the wounds (example shown in Fig. S3 in Supplementary Information). All HA-DOPA implants remained well attached, and in tight contact with the surrounding stromal tissue. After 7 days of culture, immunohistochemical staining against the human cell surface marker TRA-1-85 showed the presence of human cells both on the surface of the hydrogels as well as inside them (Fig. 7). However, we did not observe significant outgrowth of hASCs to the corneal stroma or migration of the hESC-LESCs out from the implant during this 1-week culture period. This outcome could be improved with further optimization of the implantation techniques to achieve better alignment of the implant surface with the surface of the cornea. However, we anticipate that the remodeling of the implant by the encapsulated and surrounding cells during stromal regeneration would ultimately take care of small mismatches in surface alignment between the implant and the corneal surface.

To investigate the differentiation potential of implanted hASCs in the corneal organ culture model, we adapted a method used previously for implantation of hASCs to corneal stromal wounds with HA-hydrogels, as described in Ref. [20], with known *in vitro* differentiation methods of hASCs to corneal keratocytes [11,40]. By culturing the porcine corneas with hASCs delivered in HA-DOPA or HA-HA in keratocyte differentiation medium for 10 days, we analyzed the expression of three marker genes of corneal keratocyte differentiation by qRT-PCR compared to undifferentiated hASCs. However, only one of the studied genes, lumican, was detected in satisfactory amounts after this culture period in *ex vivo* cultured hASCs as well as the 2D differentiation control (Fig. 6f). The expression of lumican in the *ex vivo* differentiated hASCs was similarly increased in HA-DOPA and HA-HA, while the expression in both gels was slightly lower than that in the 2D condition. Lumican is a small leucine rich proteoglycan aiding in ECM organization, abundantly expressed by corneal keratocytes. However, as lumican is not solely expressed by corneal cells, the differentiation of hASCs towards corneal keratocytes was not conclusively verified in this study. Despite the inconclusive keratocyte differentiation, the results suggest the 3D *ex vivo* differentiation capacity of these cells to be similar to the 2D control condition. This further strengthens the rationale behind this work, as the scope of our research focuses on the delivery of these undifferentiated cells to the corneal stroma, where their therapeutic capacity *in vivo* has been clinically demonstrated [14,15].

Based on these results, the corneal organ culture method provides the practical utility of the HA-DOPA gels as a sutureless stem cell delivery method for corneal regeneration and encourages to proceed towards *in vivo* studies for further evaluation of the therapeutic functionality of these stem cell-containing tissue adhesive implants.

## 4. Conclusions

In this study, we fabricated an implantable tissue adhesive hydrogel scaffold for the delivery of spatially compartmentalized therapeutic stem cells for simultaneous regeneration of the corneal stroma and epithelium, with encapsulated hASCs in the hydrogel bulk and hESC-LESCs on the surface. Dopamine moieties grafted to the hyaluronic acid hydrogel imparted the tissue adhesive function, facilitated the conjugation of cell-adhesive proteins to the hydrogel surface and supported hASC culture. Furthermore, incorporation of dopamine moieties augmented the cell viability, improved the mechanical properties and reduced hydrogel swelling in presence of cell culture medium. Using this sophisticated delivery system, we established the proof-of-concept of implanting two regenerative stem cell types in the cornea using a porcine corneal organ culture model, demonstrating its potential as an implantable tissue-engineered construct for corneal applications. We believe that our study represents the first sutureless delivery of any cells to the surface of the eye, as well as the first sutureless delivery system of two differentially localized cell populations to any tissue.

## Author contributions

L.K., T.I., H.S. and O.P.O. conceived the study, L.K. and M.K. designed and performed the swelling study, *in vitro* materials characterization, and cell studies and analyzed the data. S.S. and V.S.P. synthesized and characterized the hyaluronic acid derivatives, developed and characterized hydrogels, performed the rheological studies and corneal adhesion studies. S.M. contributed reagents and cell material for use in this study. L.K. and O.P.O. wrote the manuscript. M.K., T.I., S.M., and H.S. participated in critical evaluation of the manuscript.

## Conflicts of interest

The authors declare no conflict of interest.

## Data availability

All of the data reported in this work are available upon request.

## Acknowledgements

The authors would like to thank Outi Melin and Hanna Pekkanen for their assistance in producing the hESC-LESCs, and Miia Juntunen for assistance with the hASCs. We also thank the Tampere Imaging Facility (BioMediTech and Faculty of Medicine and Health Technology, Tampere University) for the imaging facilities, and Paijan Tilateurastamo for the porcine eyes. The authors thank the Graduate School of Faculty of Medicine and Life Sciences, University of Tampere,

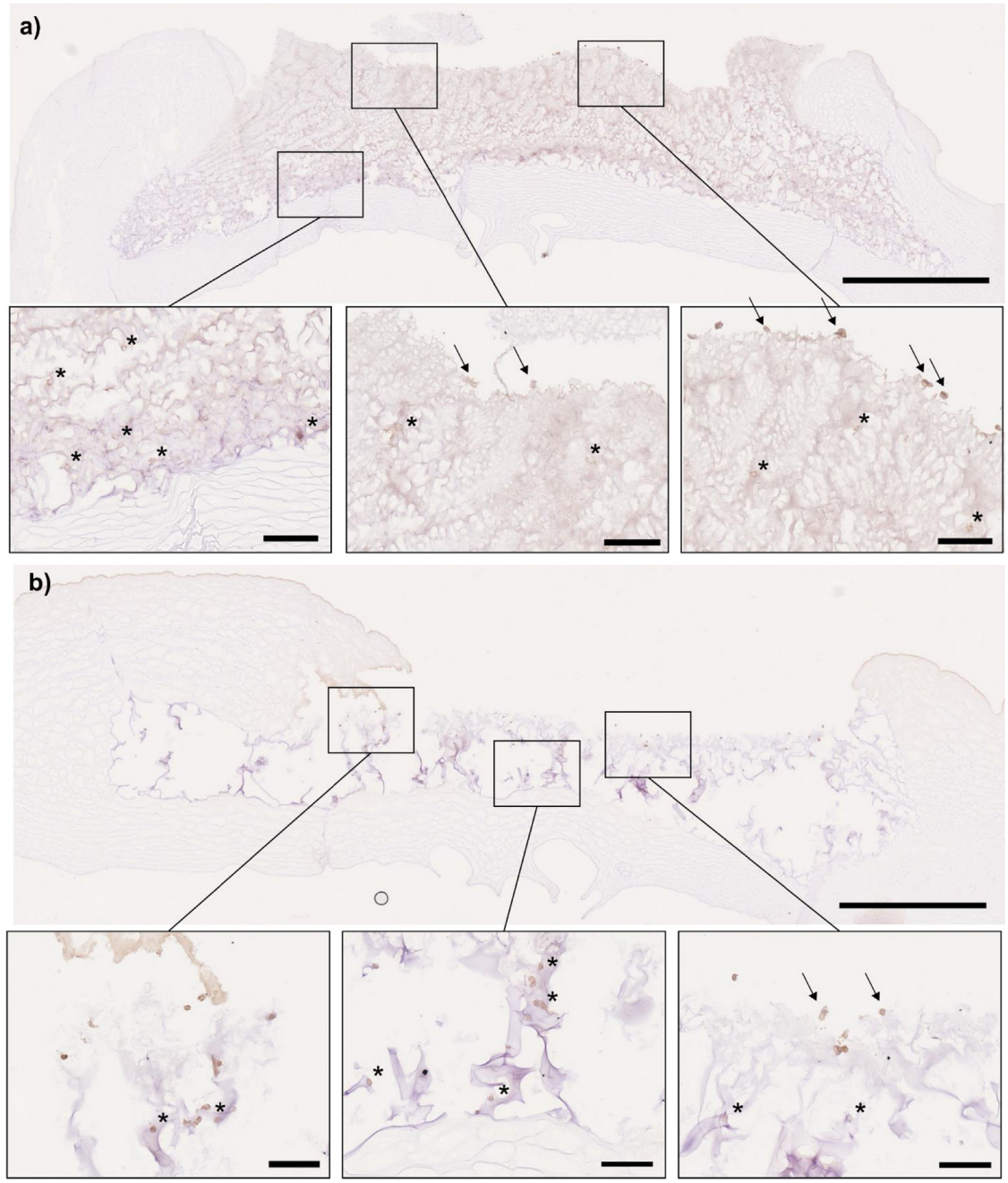


**Fig. 7.** Histological evaluation of the hASC and hESC-LESC containing HA-DOPA (a) and HA-HA (b) hydrogel implants in porcine corneal organ culture for 7 days. The presence of human cells was detected using TRA-1-85 cell surface marker (in brown). The higher magnification images show encapsulated cells (*) and cells on the surface of the implant (arrows). Scale bars in the whole cornea images are 1 mm, and 100 μm in the insets. (For interpretation of the references to color in this figure legend, the reader is referred to the Web version of this article.)

Instrumentarium Science Foundation, Academy of Finland and Business Finland for their funding for this research. This study was partly supported by the Competitive State Research Financing of the Expert Responsibility area of Tampere University Hospital.

## Appendix A. Supplementary data

Supplementary data to this article can be found online at https://doi.org/10.1016/j.biomaterials.2019.119516.

## References

[1] D. Pascolini, S.P. Mariotti, Global estimates of visual impairment: 2010, Br. J. Ophthalmol. 96 (2012) 614–618.
[2] M. Griffith, E.I. Alarcon, I. Brunette, Regenerative approaches for the cornea, J. Intern. Med. 280 (2016) 276–286.
[3] T. Nakamura, T. Inatomi, C. Sotozono, N. Koizumi, S. Kinoshita, Ocular surface reconstruction using stem cell and tissue engineering, Prog. Retin. Eye Res. 51 (2016) 187–207.
[4] G. Pellegrini, C.E. Traverso, A.T. Franzi, M. Zingirian, R. Cancedda, M. De Luca, Long-term restoration of damaged corneal surfaces with autologous cultivated corneal epithelium, Lancet 349 (1997) 990–993.
[5] S. Kolli, S. Ahmad, M. Lako, F. Figueiredo, Successful clinical implementation of corneal epithelial stem cell therapy for treatment of unilateral limbal stem cell deficiency, Stem Cells 28 (2010) 597–610.
[6] G.K. Vemuganti, S. Kashyap, V.S. Sangwan, S. Singh, Ex-vivo potential of cadaveric and fresh limbal tissues to regenerate cultured epithelium, Indian J. Ophthalmol. 52 (2004) 113.
[7] A. Mikhailova, T. Ilmarinen, H. Uusitalo, H. Skottman, Small-molecule induction promotes corneal epithelial cell differentiation from human induced pluripotent

stem cells, Stem Cell Rep. 2 (2014) 219–231.
[8] A. Mikhailova, T. Ilmarinen, A. Ratnayake, G. Petrovski, H. Uusitalo, H. Skottman, et al., Human pluripotent stem cell-derived limbal epithelial stem cells on bioengineered matrices for corneal reconstruction, Exp. Eye Res. 146 (2016) 26–34.
[9] H. Miyashita, H. Niwano, S. Yoshida, S. Hatou, E. Inagaki, K. Tsubota, et al., Long-term homeostasis and wound healing in an in vitro epithelial stem cell niche model, Sci. Rep. 7 (2017) 43557 report.
[10] J. Yang, J.W. Park, D. Zheng, R. Xu, Universal corneal epithelial-like cells derived from human embryonic stem cells for cellularization of a corneal scaffold, Transl. Vis. Sci. Technol. 7 (2018) 23.
[11] Y. Du, D.S. Roh, M.L. Funderburgh, M.M. Mann, K.G. Marra, J.P. Rubin, et al., Adipose-derived stem cells differentiate to keratocytes in vitro, Mol. Vis. 16 (2010) 2680–2689.
[12] L. Zhang, V.J. Coulson-Thomas, T.G. Ferreira, W.W.Y. Kao, Mesenchymal stem cells for treating ocular surface diseases, BMC Ophthalmol. 15 (2015) 155.
[13] S. Zhang, L. Espandar, K.M. Imhof, B.A. Bunnell, Differentiation of human adipose-derived stem cells along the keratocyte lineage, J. Clin. Exp. Ophthalmol. 4 (2013) 11435.
[14] F. Arnalich-Montiel, S. Pastor, A. Blazquez-Martinez, J. Fernandez-Delgado, M. Nistal, Alio del Barrio, L. Jorge, et al., Adipose-derived stem cells are a source for cell therapy of the corneal stroma, Stem Cells 26 (2008) 570–579.
[15] Alió del Barrio, L. Jorge, M. El Zarif, M.P. de Miguel, A. Azaar, N. Makdissy, W. Harb, et al., Cellular therapy with human autologous adipose-derived adult stem cells for advanced keratoconus, Cornea 36 (2017) 952–960.
[16] A. Sorkio, L. Koch, L. Koivusalo, A. Deiwick, S. Miettinen, B. Chichkov, et al., Human stem cell based corneal tissue mimicking structures using laser-assisted 3D bioprinting and functional bioinks, Biomaterials 171 (2018) 57–71.
[17] L.J. Bray, K.A. George, S. Suzuki, T.V. Chirila, D.G. Harkin, Fabrication of a corneal-limbal tissue substitute using silk fibroin, in: B. Wright, C. Connon (Eds.), Corneal Regenerative Medicine, Springer, 2013, pp. 165–178.
[18] M. González-Andrades, R. Mata, M. del Carmen González-Gallardo, S. Medialdea, S. Arias-Santiago, J. Martínez-Atienza, et al., A study protocol for a multicentre randomised clinical trial evaluating the safety and feasibility of a bioengineered human allogeneic nanostructured anterior cornea in patients with advanced corneal trophic ulcers refractory to conventional treatment, BMJ open 7 (2017) e016487.
[19] O.P. Oommen, S. Wang, M. Kisiel, M. Sloff, J. Hilborn, O.P. Varghese, Smart design of stable extracellular matrix mimetic hydrogel: synthesis, characterization, and in vitro and in vivo evaluation for tissue engineering, Adv. Funct. Mater. 23 (2013) 1273–1280.
[20] L. Koivusalo, J. Karvinen, E. Sorsa, I. Jönkkäri, J. Väliaho, P. Kallio, et al., Hydrazone crosslinked hyaluronan-based hydrogels for therapeutic delivery of adipose stem cells to treat corneal defects, Mater. Sci. Eng. C 85 (2018) 68.
[21] E. Martínez-Sanz, D.A. Ossipov, J. Hilborn, S. Larsson, K.B. Jonsson, O.P. Varghese, Bone reservoir: injectable hyaluronic acid hydrogel for minimal invasive bone augmentation, J. Control. Release 152 (2011) 232–240.
[22] D.A. Ossipov, S. Piskounova, O.P. Varghese, J. Hilborn, Functionalization of hyaluronic acid with chemoselective groups via a disulfide-based protection strategy for in situ formation of mechanically stable hydrogels, Biomacromolecules 11 (2010) 2247–2254.
[23] T.F. Gesteira, M. Sun, Y.M. Coulson-Thomas, Y. Yamaguchi, L. Yeh, V. Hascall, et al., Hyaluronan rich microenvironment in the limbal stem cell niche regulates limbal stem cell differentiation, Investig. Ophthalmol. Vis. Sci. 58 (2017) 4407–4421.
[24] J.A. Gomes, R. Amankwah, A. Powell-Richards, H.S. Dua, Sodium hyaluronate (hyaluronic acid) promotes migration of human corneal epithelial cells in vitro, Br. J. Ophthalmol. 88 (2004) 821–825.
[25] C. Fiorica, R.A. Senior, G. Pitarresi, F.S. Palumbo, G. Giammona, P. Deshpande, et al., Biocompatible hydrogels based on hyaluronic acid cross-linked with a polyaspartamide derivative as delivery systems for epithelial limbal cells, Int. J. Pharm. 414 (2011) 104–111.
[26] L. Espandar, B. Bunnell, G.Y. Wang, P. Gregory, C. McBride, M. Moshirfar, Adipose-derived stem cells on hyaluronic acid–derived scaffold: a new horizon in bioengineered cornea, Arch. Ophthalmol. 130 (2012) 202–208.
[27] P.J.M. Bouten, M. Zonjee, J. Bender, S.T.K. Yauw, H. van Goor, Hest van, C.M. Jan, et al., The chemistry of tissue adhesive materials, Prog. Polym. Sci. 39 (2014) 1375–1405.
[28] J. Shin, J.S. Lee, C. Lee, H. Park, K. Yang, Y. Jin, et al., Tissue adhesive catechol-modified hyaluronic acid hydrogel for effective, minimally invasive cell therapy, Adv. Funct. Mater. 25 (2015) 3814–3824.
[29] C.E. Brubaker, H. Kissler, L. Wang, D.B. Kaufman, P.B. Messersmith, Biological performance of mussel-inspired adhesive in extrahepatic islet transplantation, Biomaterials 31 (2010) 420–427.
[30] Y. Lee, H.J. Chung, S. Yeo, C. Ahn, H. Lee, P.B. Messersmith, et al., Thermo-sensitive, injectable, and tissue adhesive sol–gel transition hyaluronic acid/pluronic composite hydrogels prepared from bio-inspired catechol-thiol reaction, Soft Matter 6 (2010) 977–983.
[31] Y. Chan Choi, J.S. Choi, Y.J. Jung, Y.W. Cho, Human gelatin tissue-adhesive hydrogels prepared by enzyme-mediated biosynthesis of DOPA and Fe3+ion cross-linking, J. Mater. Chem. B 2 (2014) 201–209.
[32] F. Scognamiglio, A. Travan, M. Borgogna, I. Donati, E. Marsich, J.W.A.M. Bosmans, et al., Enhanced bioadhesivity of dopamine-functionalized polysaccharidic membranes for general surgery applications, Acta Biomater. 44 (2016) 232–242.
[33] L. Figueira, C. Ferreira, C. Janeiro, P. Serrao, F. Falcao-Reis, D. Moura, Concentration gradient of noradrenaline from the periphery to the centre of the cornea - a clue to its origin, Exp. Eye Res. 168 (2018) 107–114.
[34] O.P. Varghese, M. Kisiel, E. Martínez-Sanz, D.A. Ossipov, J. Hilborn, Synthesis of guanidinium-modified hyaluronic Acid hydrogel, Macromol. Rapid Commun. 31 (2010) 1175–1180.
[35] S. Wang, O.P. Oommen, H. Yan, O.P. Varghese, Mild and efficient strategy for site-selective aldehyde modification of glycosaminoglycans: tailoring hydrogels with tunable release of growth factor, Biomacromolecules 14 (2013) 2427–2432.
[36] J.M. Gimble, F. Guilak, Adipose-derived adult stem cells: isolation, characterization, and differentiation potential, Cytotherapy 5 (2003) 362–369.
[37] B. Lindroos, S. Boucher, L. Chase, H. Kuokkanen, H. Huhtala, R. Haataja, et al., Serum-free, xeno-free culture media maintain the proliferation rate and multipotentiality of adipose stem cells in vitro, Cytotherapy 11 (2009) 958–972.
[38] H. Hongisto, T. Ilmarinen, M. Vattulainen, A. Mikhailova, H. Skottman, Xeno- and feeder-free differentiation of human pluripotent stem cells to two distinct ocular epithelial cell types using simple modifications of one method, Stem Cell Res. Ther. 8 (2017) 291.
[39] Heli Skottman, Derivation and characterization of three new human embryonic stem cell lines in Finland, Vitro Cell Dev Biol : Anim, vol. 46, 2010, pp. 206–209.
[40] A.P. Lynch, M. Ahearne, Retinoic acid enhances the differentiation of adipose-derived stem cells to keratocytes in vitro, Transl. Vis. Sci. Technol. 6 (2017) 6.
[41] P.B. Welzel, S. Prokoph, A. Zieris, M. Grimmer, S. Zschoche, U. Freudenberg, et al., Modulating biofunctional starPEG heparin hydrogels by varying size and ratio of the constituents, Polymers 3 (2011) 602–620.
[42] S.J. Petsche, D. Chernyak, J. Martiz, M.E. Levenston, P.M. Pinsky, Depth-dependent transverse shear properties of the human corneal stroma, Investig. Ophthalmol. Vis. Sci. 53 (2012) 873–880.
[43] P. Fagerholm, N.S. Lagali, J.A. Ong, K. Merrett, W.B. Jackson, J.W. Polarek, et al., Stable corneal regeneration four years after implantation of a cell-free recombinant human collagen scaffold, Biomaterials 35 (2014) 2420–2427.
[44] S.M. Lam, L. Tong, X. Duan, A. Petznick, M.R. Wenk, G. Shui, Extensive characterization of human tear fluid collected using different techniques unravels the presence of novel lipid amphiphiles, J. Lipid Res. 55 (2014) 289–298.
[45] S.L. Wilson, I. Wimpenny, M. Ahearne, S. Rauz, A.J. El Haj, Y. Yang, Chemical and topographical effects on cell differentiation and matrix elasticity in a corneal stromal layer model, Adv. Funct. Mater. 22 (2012) 3641–3649.
[46] D. Wang, S. Varghese, B. Sharma, I. Strehin, S. Fermanian, J. Gorham, et al., Multifunctional chondroitin sulphate for cartilage tissue–biomaterial integration, Nat. Mater. 6 (2007) 385.
[47] O.P. Oommen, J. Garousi, M. Sloff, O.P. Varghese, Tailored doxorubicin-H yaluronan conjugate as a potent anticancer glyco-D rug: an alternative to prodrug approach, Macromol. Biosci. 14 (2014) 327–333.
[48] K.M. Meek, C. Knupp, Corneal structure and transparency, Prog. Retin. Eye Res. 49 (2015) 1–16.
[49] Y. Liu, K. Ai, L. Lu, Polydopamine and its derivative materials: synthesis and promising applications in energy, environmental, and biomedical fields, Chem. Rev. 114 (2014) 5057–5115.
[50] Silvia A. Ferreira, Meghna S. Motwani, Peter A. Faull, Alexis J. Seymour, Tracy T.L. Yu, Marjan Enayati, et al., Bi-directional cell-pericellular matrix interactions direct stem cell fate, Nat. Commun. 9 (2018) 1–12.
[51] C. Loebel, R.L. Mauck, J.A. Burdick, Local nascent protein deposition and remodelling guide mesenchymal stromal cell mechanosensing and fate in three-dimensional hydrogels, Nat. Mater. 1 (2019).
[52] K. Merrett, C.M. Griffith, Y. Deslandes, G. Pleizier, H. Sheardown, Adhesion of corneal epithelial cells to cell adhesion peptide modified pHEMA surfaces, J. Biomater. Sci. Polym. Ed. 12 (2001) 647–671.
[53] D. Bermejo-Velasco, G.N. Nawale, O.P. Oommen, J. Hilborn, O.P. Varghese, Thiazolidine chemistry revisited: a fast, efficient and stable click-type reaction at physiological pH, Chem. Commun. 54 (2018) 12507–12510.